Published by IOP Publishing for Sissa Medialab

Received: *November 14, 2022*
Accepted: *January 16, 2023*
Published: *February 13, 2023*

Analysis of humidity sensitivity of silicon strip sensors for ATLAS upgrade tracker, pre- and post-irradiation

J. Fernández-Tejero,[a,b,*] **A. Affolder,**[c] **E. Bach,**[d] **M.J. Basso,**[e] **A. Bhardwaj,**[e] **V. Cindro,**[f] **A. Dowling,**[c] **V. Fadeyev,**[c] **C. Fleta,**[d] **A. Fournier,**[a,b] **K. Hara,**[g] **A. Howe,**[e] **C. Jessiman,**[h] **J. Keller,**[h] **D. Kisliuk,**[e] **C. Klein,**[h] **T. Koffas,**[h] **J. Kroll,**[i] **V. Latonova,**[i,j] **K. Mahtani,**[e] **I. Mandić,**[f] **F. Martinez-Mckinney,**[c] **M. Mikestikova,**[i] **K. Nakamura,**[k] **R.S. Orr,**[e] **L. Poley,**[a,b] **E. Staats,**[h] **B. Stelzer,**[a,b] **J. Suzuki,**[g] **M. Ullán,**[d] **Y. Unno,**[k] **J. Yarwick,**[c] **I. Zatocilova**[i] **and Y. Zhou**[e]

[a] *Department of Physics, Simon Fraser University, 8888 University Drive, Burnaby, B.C. V5A 1S6, Canada*
[b] *TRIUMF, 4004 Wesbrook Mall, Vancouver, B.C. V6T 2A3, Canada*
[c] *Santa Cruz Institute for Particle Physics (SCIPP), University of California, Santa Cruz, CA 95064, U.S.A.*
[d] *Instituto de Microelectrónica de Barcelona (IMB-CNM, CSIC), Campus UAB-Bellaterra, 08193 Barcelona, Spain*
[e] *Department of Physics, University of Toronto, 60 Saint George St., Toronto, Ontario M5S1A7, Canada*
[f] *Experimental Particle Physics Department, Jožef Stefan Institute, Jamova 39, SI-1000 Ljubljana, Slovenia*
[g] *Institute of Pure and Applied Sciences, University of Tsukuba, 1-1-1 Tennodai, Tsukuba, Ibaraki 305-8571, Japan*
[h] *Physics Department, Carleton University, 1125 Colonel By Drive, Ottawa, Ontario, K1S 5B6, Canada*
[i] *Academy of Sciences of the Czech Republic, Institute of Physics, Na Slovance 2, 18221 Prague 8, Czech Republic*
[j] *Faculty of Mathematics and Physics, Charles University, V Holesovickach 2, Prague, CZ18000, Czech Republic*
[k] *Institute of Particle and Nuclear Study, High Energy Accelerator Research Organization (KEK), 1-1 Oho, Tsukuba, Ibaraki 305-0801, Japan*

E-mail: Xavi.Fdez@cern.ch

[*] Corresponding author.

https://doi.org/10.1088/1748-0221/18/02/P02012

2023 JINST 18 P02012

Abstract: During the prototyping phase of the new ATLAS Inner-Tracker (ITk) strip sensors, a degradation of the device breakdown voltage at high humidity was observed. Although the degradation was temporary, showing a fast recovery in dry conditions, the study of the influence of humidity on the sensor performance was critical to establish counter-measures and handling protocols during production testing in order to ensure the proper performance of the upgraded detector.

The work presented here has the objective to study for the first time the breakdown voltage deterioration in presence of ambient humidity of ATLAS ITk production-layout strip sensors with different surface properties, before and after proton, neutron and gamma irradiations. A study of the humidity sensitivity of miniature ATLAS ITk strip sensors, before and after proton irradiations, is also presented to compare the sensitivity of devices with different sizes.

The sensors were also exposed for several days to high humidity with the aim to recreate and evaluate the influence of the detector integration environment expected during the Large Hadron Collider (LHC) Long Shutdown 3 (LS3) in 2026, where the sensors will be exposed to ambient humidity for prolonged times.

Keywords: Particle tracking detectors (Solid-state detectors); Radiation-hard detectors; Si microstrip and pad detectors; Solid state detectors

2023 JINST 18 P02012

Contents

1 Framework **1**

2 Humidity sensitivity **2**
- 2.1 Breakdown voltage dependence 2
- 2.2 High humidity exposure 3
- 2.3 Influence of irradiation 3

3 Devices under test **3**
- 3.1 Non irradiated sensors 4
- 3.2 Sensors irradiated with protons, neutrons and gammas 4

4 Results **5**
- 4.1 Humidity sensitivity non-irradiated full-size sensors 5
- 4.2 Humidity sensitivity irradiated full-size sensors 7
- 4.3 Humidity sensitivity of miniature sensors 9

5 Conclusions **10**

2023 JINST 18 P02012

1 Framework

The ATLAS collaboration is working on a major upgrade of the current Semiconductor Tracker (SCT) [1], that will be replaced by the new Inner-Tracker (ITk) [2], able to withstand the extreme operational conditions expected for the forthcoming High-Luminosity Large Hadron Collider (HL-LHC) upgrade [3]. During the prototyping phase of the new large area silicon strip sensors, the community observed a degradation of the breakdown voltage when the devices with final technology options were exposed to high humidity, recovering the electrical performance prior to the exposure after a short period in dry conditions [4, 5]. These findings helped to understand the humidity sensitivity of the new sensors, defining the optimal working conditions and handling recommendations during production testing.

In 2020, the ATLAS strip sensor community started the pre-production phase [6], receiving the first sensors fabricated by Hamamatsu Photonics K.K. (HPK) using the final layout design. The work presented here is focused on the analysis of the humidity sensitivity of production-layout sensors with different surface properties and miniature sensors, before and after irradiation, providing new results on their influence on the humidity sensitivity.

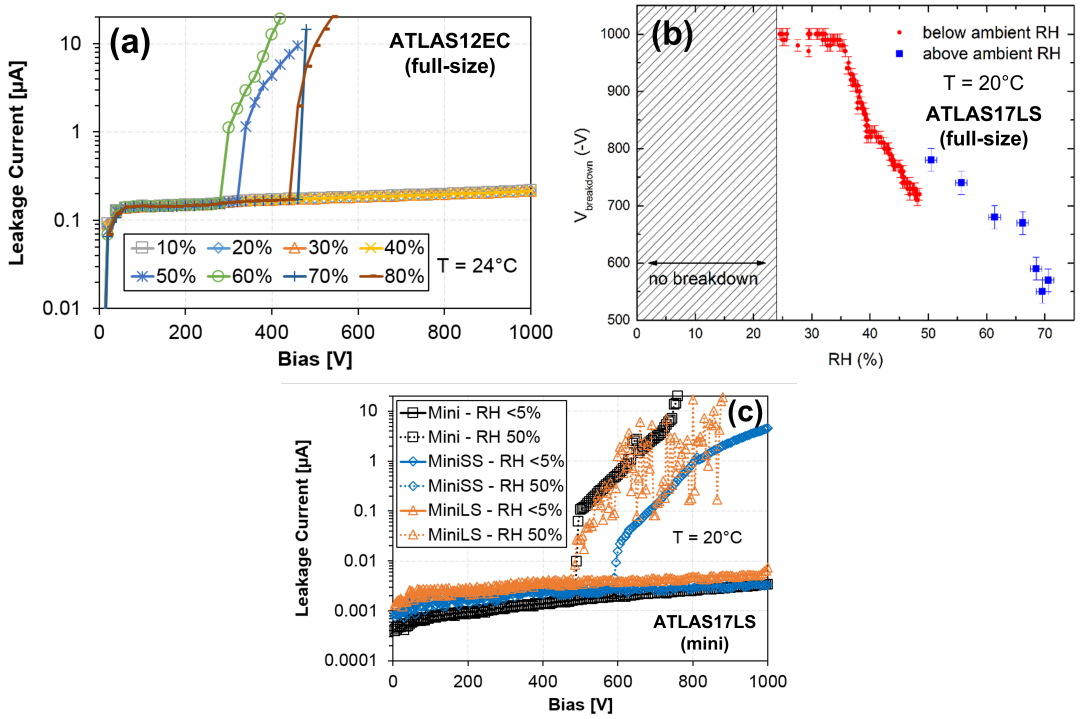

Figure 1. (a) Reverse leakage current of an ATLAS12EC large area prototype at different humidity conditions, (b) breakdown voltage dependence with humidity of an ATLAS17LS prototype, and (c) reverse leakage current of ATLAS17LS miniature sensors at different humidity conditions. Figures adapted from [4].

2 Humidity sensitivity

2.1 Breakdown voltage dependence

During the prototyping phase, participating institutes reported a degradation of the breakdown voltage when the leakage current of End-cap ATLAS12EC (figure 1(a)) and Barrel ATLAS17LS (figure 1(b)) prototype sensors, fabricated by HPK and Infineon Technologies AG, was measured at ambient humidity conditions. A similar degradation of the breakdown voltage was observed on miniature sensors (figure 1(c)) with identical edge structures (bias/guard/edge rings) but smaller active areas. Although the results obtained were similar, a smaller fraction of the miniature sensors showed a clear dependence on humidity variations, revealing less frequent incidence of humidity sensitivity on smaller devices [4]. The sensor community started an extensive investigation campaign, accumulating more evidences of the inverse relation between relative humidity and sensor breakdown voltage.

Several palliative treatments were attempted, observing a fast recovery of the sensor performance in dry storage, and after baking or cleaning treatments. Although the recovery of the sensor performance was demonstrated, the reduction of breakdown voltage when the sensors were biased at high humidity was not mitigated. Thermal images of sensors in breakdown behaviour at high humidity revealed hotspots in the sensor edge, suggesting that the separation between guard/edge ring structures in combination with the passivation thickness could be responsible for the humidity sensitivity. The hypothesis proposed was that, in presence of high humidity, the surface of the sensor

2023 JINST 18 P02012

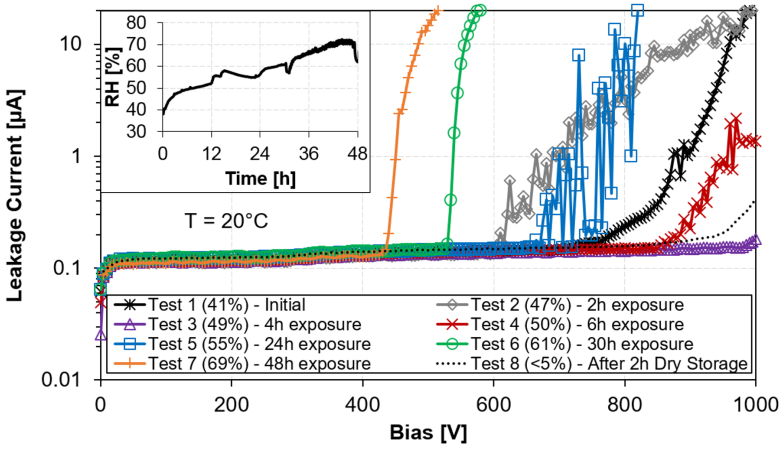

Figure 2. Breakdown voltage degradation of a prototype ATLAS17LS full-size sensor exposed to high humidity (inner plot) for 48h. Last measurement (Test 8) performed at low humidity. Figure adapted from [4].

accumulates positive hydrogen ions, inducing the appearance of electron/hole inversion/accumulation layers between the n+ and p+ implants of the guard ring and dicing edge, respectively, causing the premature breakdown when the device is biased at high humidity.

2.2 High humidity exposure

With the objective to evaluate the risks of permanent degradation of sensors exposed to high humidity, biased and unbiased prototype sensors were exposed to high humidity for several days [4]. The experiment demonstrated that sensors biased over the breakdown voltage can develop permanent damages when exposed to high humidity for long periods of time, but unbiased sensors show only a temporary degradation, recovering the performance prior to the exposure after hours/days in dry conditions (figure 2).

2.3 Influence of irradiation

While at the prototyping phase the influence of the irradiation on the humidity sensitivity was unclear, a first study of an ATLAS12EC prototype sensor irradiated with protons up to 5×10^{14} n_{eq}/cm^2 showed no breakdown below 1 kV at high humidity (50%) and low temperature (−20°C) (figure 3). These results with an early full-size prototype suggested for the first time a progressive mitigation of the humidity sensitivity for the high radiation environment expected for the HL-LHC.

3 Devices under test

With the aim to investigate the humidity sensitivity of production-layout ATLAS ITk silicon strip sensors, several miniature and full-size sensors were selected during the prototype and pre-production phases, respectively. Additionally, HPK fabricated a special batch with different surface properties. Some of these sensors were irradiated to different fluences of protons, or neutrons+gammas, up to fluences expected at the end of the HL-LHC lifetime.

2023 JINST 18 P02012

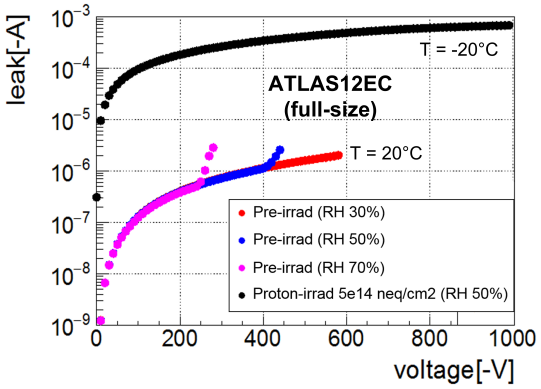

Figure 3. Prototype ATLAS12EC full-size sensor irradiated with protons up to 5×10^{14} n_{eq}/cm^2 shows no breakdown voltage below 1 kV at high humidity (50%) and low temperature (−20°C).

Table 1. Sensor types and process modifications applied to study the humidity sensitivity.

	Sensor Type	Special Treatment	Additional Treatment	Special Masking	Thicker Passivation	p-spray Addition (target value, cm^{-2})
Prototype	Mini					
Type A (production)	Full-size	X				
Type A′	Full-size	X	X			
Type B	Full-size	X		X		
Type C	Full-size	X			X	
Type D high	Full-size	X				8×10^{11}
Type D low	Full-size	X				4×10^{11}

The full-size ($\sim 10 \times 10\,cm^2$) sensors used in this work are pre-production ATLAS Barrel Short-Strip (SS) sensors with final layout designs for HL-LHC, also called ATLAS18SS [6]. The miniature sensors ($\sim 1 \times 1\,cm^2$) were fabricated by HPK during the prototyping phase, included as test structures in the wafer layout of the ATLAS17LS prototype [8]. All the sensors are n^+-on-p type with a thickness of 320 µm. The active area of the full-size sensors is divided in 4 segments containing 1,282 parallel strips per segment with a strip length of 24,155 µm and a strip pitch of 75.5 µm. While the active area of the miniature sensors has only one segment containing 104 parallel strips with a strip length of 8,000 µm and same strip pitch as full-size sensors.

3.1 Non irradiated sensors

In total, full-size sensors with 6 different surface characteristics were used for the study before irradiation, coming from the special batch fabricated by HPK. Table 1 shows the different process modifications applied, in comparison with the default production technology (Type A).

3.2 Sensors irradiated with protons, neutrons and gammas

With the objective to study the evolution of the humidity sensitivity in working conditions, several production-like full-size sensors (Type A) were irradiated to 3 different low proton fluences (1×10^{13}, 5×10^{13}, 1×10^{14} n_{eq}/cm^2), and several prototype miniature sensors were irradiated to 4 different

2023 JINST 18 P02012

Table 2. Proton and neutron+gamma irradiations applied to each sensor type.

	Sensor Type	Proton irrad (n_{eq}/cm^2)	Neutron+Gamma irrad (n_{eq}/cm^2 + Mrad)
Prototype	Mini	1×10^{14}, 5×10^{14}, 1×10^{15}, 2×10^{15}	
Type A (production)	Full-size	1×10^{13}, 5×10^{13}, 1×10^{14}	
Type A′	Full-size		
Type B	Full-size		
Type C	Full-size		$1.6 \times 10^{15} + 66$
Type D high	Full-size		$1.6 \times 10^{15} + 66$
Type D low	Full-size		$1.6 \times 10^{15} + 66$

high proton fluences (1×10^{14}, 5×10^{14}, 1×10^{15}, 2×10^{15} n_{eq}/cm^2). Additionally, full-size sensors with different passivation thickness (Type C) and p-spray addition (Type D high/low) were irradiated with neutrons (1.6×10^{15} n_{eq}/cm^2) and gammas (66 Mrad) up to fluences expected at the end of the HL-LHC lifetime. Table 2 shows the different irradiations and fluences applied to each sensor type.

4 Results

This section shows and discusses the IV characteristics of the sensors measured at different relative humidity, before and after irradiation. Additionally, all the full-size sensors were exposed to high humidity unbiased, for several days to study its influence.

4.1 Humidity sensitivity non-irradiated full-size sensors

For the study before irradiation, the leakage current was measured up to 1 kV at room temperature (20°C). For each sensor, a first IV was performed at low humidity (< 10%), followed by a second IV at standard cleanroom humidity (35–45%), a third IV at high humidity (50–60%) and again several consecutive measurements at low humidity to study the recovery of the sensors when tested in dry conditions, also called "training". Each measurement took around 10 minutes and the time between the measurements was less than 20 minutes. Finally, in order to study the influence of the exposure to high humidity, all the full-size sensors were exposed, unbiased, to 30–50% humidity for 40 hours, and measured again at low humidity.

Figure 4 shows the IV curves obtained for each sensor, and for each step detailed above. To facilitate the comparison, table 3 summarizes the measured breakdown voltage for all the cases and training needed to recover the sensors at low humidity.

Initially, at low humidity, all sensor types show breakdown voltages higher than 1 kV, and low and stable leakage current. For reference, the ATLAS specifications establish that sensors measured at low humidity with breakdown voltage above 500 V and leakage current at 500 V below 0.1 $\mu A/cm^2$ are considered good sensors. Then, all the sensor types show IV characteristics at low humidity fulfilling the requirements imposed by ATLAS.

At cleanroom humidity (35–45%), all the sensor types show a clear deterioration of the breakdown voltage. In particular, the sensor with special masking (figure 4(c)) shows the lowest breakdown voltage, 570 V in cleanroom conditions. On the other hand, the sensor with a low dose

2023 JINST 18 P02012

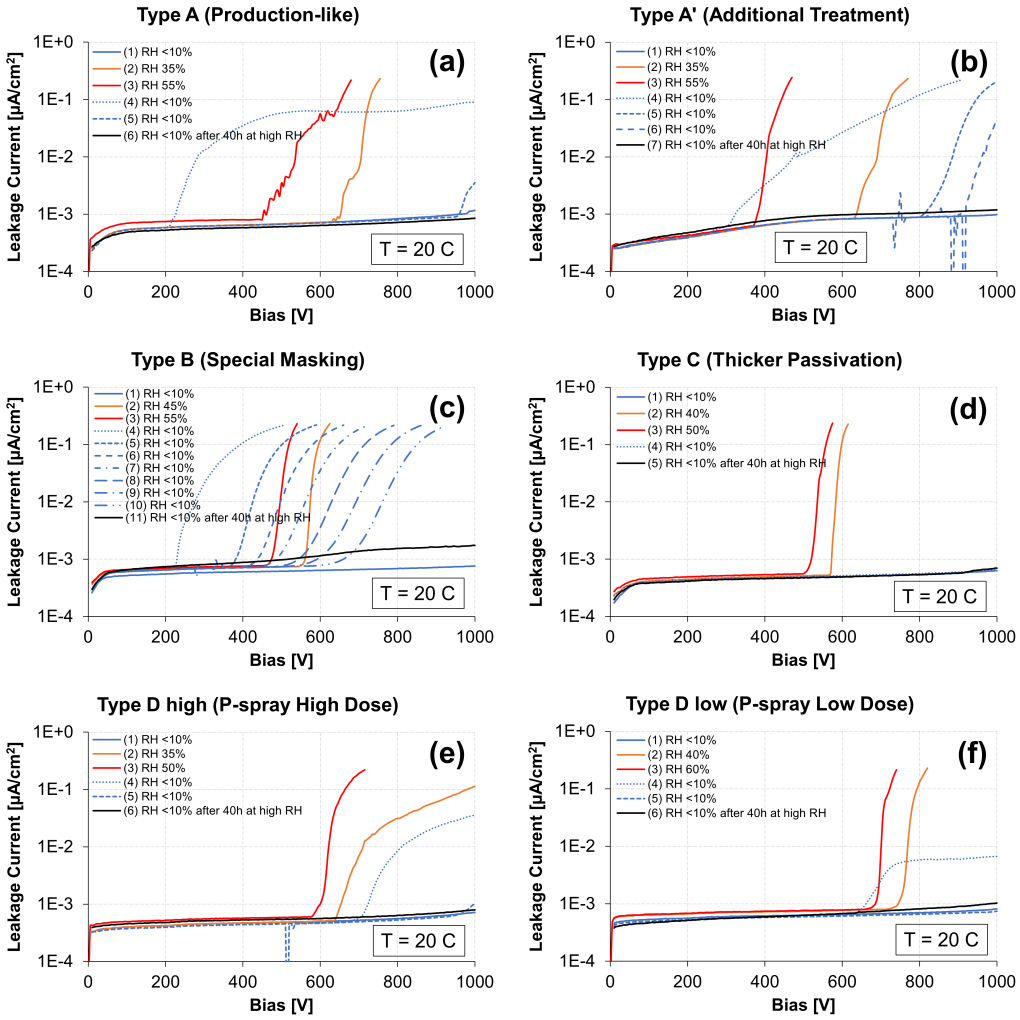

Figure 4. IV curves at different RH and after 40 h exposure to high humidity for all full-size sensor before irradiation: (a) Type A, (b) Type A', (c) Type B, (d) Type C, (e) Type D high and (f) Type D low.

Table 3. Breakdown voltage at different RH, training effect and influence of 40 h exposure to high humidity for all full-size sensor types before irradiation.

	Breakdown at Low RH (<10%)	Breakdown at Cleanroom RH (35–45%)	Breakdown at High RH (50–60%)	IVs at low RH needed to recover (training)	Breakdown after 40 h exposure (30–50%)
Type A (production)	> 1 kV	650 V	450 V	2–3 IVs	> 1 kV
Type A′	> 1 kV	640 V	380 V (Worst)	3–4 IVs	> 1 kV
Type B	>1 kV	570 V (Worst)	470 V	> 7 IVs (Worst)	> 1 kV
Type C	>1 kV	580 V	520 V	1 IV (Best)	> 1 kV
Type D high	>1 kV	640 V	590 V	2–3 IVs	> 1 kV
Type D low	>1 kV	760 V (Best)	680 V (Best)	2 IVs	> 1 kV

2023 JINST 18 P02012

of p-spray (figure 4(f)) shows the best results with a breakdown voltage of 760 V. However, all the sensor types still show breakdown voltages above 500 V, fulfilling the ATLAS specifications.

As expected, at high humidity (50–60%) the deterioration of the breakdown voltage is even higher. The sensor with additional treatment (figure 4(b)) has the lowest breakdown at 380 V, and again the sensor with a low dose of p-spray (figure 4(f)) shows the best results, keeping the breakdown voltage at 680 V even at high humidity. At these humidity conditions, only the sensors with thicker passivation (Type C) or p-spray addition (Type D low and high) still fulfill the ATLAS specifications, showing breakdown voltages above 500 V.

All the sensors were measured again at low humidity several consecutive times (training), showing improved breakdown voltages after each new measurement. In general terms, all the sensors showed a fast recovery, needing only 1–3 consecutive IVs to show again a breakdown voltage above 900 V. However, the sensor with special masking (figure 4(c)) was not recovered, even after 7 IVs.

Finally, the sensors were exposed unbiased to high humidity (30-50%) during 40 hours, and measured again at low humidity (< 10%) after the exposure. Similarly to the results obtained with prototyping sensors (figure 2), the breakdown voltage was not influenced by the exposure to high humidity if the devices were stored unbiased.

As suggested in [4], positive charges can be accumulated in the passivation layers in presence of humidity due to the fact that electrons can move easily in the oxides under the applied potential. Then, the presence of these positive charges in the passivation-air interface could lead to the formation of a conducting electron inversion layer in the silicon-oxide interface, extending the guard ring potential towards the sensor edge and reducing the breakdown voltage of the device. This hypothesis seems to be reinforced by the good results obtained with sensors with thicker passivation or p-spray addition. At a given humidity condition, thicker passivation layers can reduce the influence of the positive charges in the creation of conducting electron inversion layers, requiring higher humidity to deteriorate the breakdown voltage. Similarly, the addition of p-spray to the silicon bulk surface can help to minimize the accumulation of positive charges in presence of humidity, requiring higher humidity to deteriorate the breakdown voltage. Although none of these solutions seem to completely mitigate the humidity sensitivity, the results indicate that the breakdown voltage is less influenced by humidity when the sensors have thicker passivation layers or p-spray treatments.

4.2 Humidity sensitivity irradiated full-size sensors

For the study of the humidity sensitivity of irradiated full-size sensors, the leakage current was measured using a manual probe station connected to a nitrogen line to control the relative humidity inside the chamber, and with the chuck at −20°C. The production-like (Type A) sensors irradiated to low fluences (1×10^{13}, 5×10^{13} and 1×10^{14} n_{eq}/cm^2) were measured up to 700 V, while the sensors with thicker passivation (Type C) and p-spray addition (Type D high/low) irradiated to high fluences with neutrons (1.6×10^{15} n_{eq}/cm^2) and gammas (66 Mrad) were measured up to 500 V. The relative humidity was controlled by modifying the nitrogen flux, and monitored using a digital temperature and humidity (T/RH) sensor located around 5 cm above the sensor surface. Due to the distance between the T/RH sensor and the chuck, the temperature of the T/RH sensor was several degrees Celsius higher than the sensor surface, and the humidity readings were only used in this case as an indicative of low or high humidity when the nitrogen flow is open or closed, with set points of 1% and 40% RH humidity, respectively. Then, due to these setup limitations, the precise control

2023 JINST 18 P02012

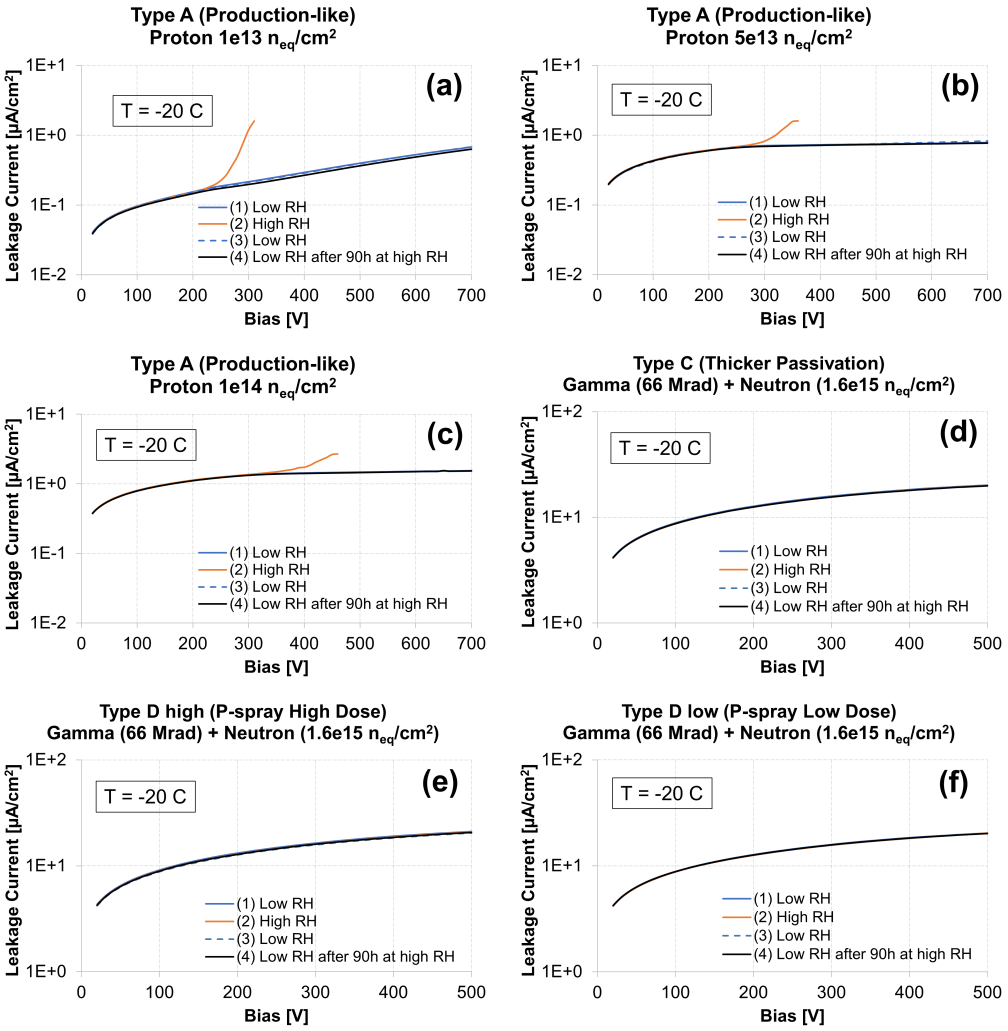

Figure 5. IV curves at different RH and after 90h exposure to high humidity for full-size sensors irradiated with protons and neutrons+gammas: (a) Type A (protons 1×10^{13} n_{eq}/cm^2), (b) Type A (protons 5×10^{13} n_{eq}/cm^2), (c) Type A (protons 1×10^{14} n_{eq}/cm^2), (d) Type C (neutrons 1.6×10^{15} n_{eq}/cm^2 + gammas 66 Mrad), (e) Type D high (neutrons 1.6×10^{15} n_{eq}/cm^2 + gammas 66 Mrad) and (f) Type D low (neutrons 1.6×10^{15} n_{eq}/cm^2 + gammas 66 Mrad).

of the dew point was not possible, observing condensation (ice) on the sensor surface during the measurements at low temperature and high humidity.

The leakage current was initially measured at low humidity (< 10%), followed by a measurement at high humidity, and again at low humidity to study the recovery. All the irradiated sensors were annealed for 80 minutes at 60°C before the measurements. Finally, all the sensors were exposed 90 hours to 40–60% humidity at 20°C, and measured again at low humidity to study the influence of the exposure. Figure 5 shows the IV curves obtained for all the irradiated full-size sensors and for all the steps detailed above.

Production-like sensors irradiated to low fluences (figure 5(a), (b) and (c)) show no breakdown below 700 V at low humidity. However, at high humidity the breakdown voltage was reduced

2023 JINST 18 P02012

to 250 V, 300 V and 350 V for the sensors irradiated to 1×10^{13}, 5×10^{13} and 1×10^{14} n_{eq}/cm^2, respectively. However, the breakdown voltage was rapidly recovered at low humidity for the three fluences, showing no breakdown below 700 V for the first IV performed after the measurement at high humidity. Similarly to the observed for non-irradiated sensors, 90 hours of exposure to high humidity had no effect on the IV characteristics, showing identical curves and no breakdown below 700 V at low humidity, before and after exposure.

Similarly to production-like sensors irradiated to low fluences, sensors with thicker passivation or p-spray addition irradiated to high fluences show no breakdown below 500 V at low humidity (figure 5(d), (e) and (f)). However, in this case even at high humidity no breakdown is observed below 500 V, confirming a progressive reduction of the humidity sensitivity while the sensors accumulate more fluence and the eventual mitigation for fluences above 1.6×10^{15} n_{eq}/cm^2. As observed for lower fluences and non-irradiated sensors, the exposure of 90 hours to high humidity had no effect on the breakdown voltage at low humidity, showing identical IV curves before and after the exposure. These measurements also demonstrate that thicker passivation or p-spray addition have no influence on the leakage current after irradiation, showing identical curves for the different surface properties.

4.3 Humidity sensitivity of miniature sensors

The study of prototype miniature sensors was performed using a custom box with dry air supply, installed in a freezer. Similarly to the setup for the full-size sensors, the temperature and humidity conditions were monitored using a digital T/RH sensor, but located only 1 cm above the sample surface. Since the setup (box) was inside a freezer, in this case the temperature of the sample and the T/RH sensor are virtually the same, and precise values of RH were obtained for the study of miniature sensors, keeping always the sample above the dew point.

The leakage current was measured up to 500 V before irradiation, and up to 700 V after irradiation, with the sensors exposed to different humidity conditions ranging from 3 to 78%. The measurements before irradiation were performed at ambient temperature (23 ± 1°C), and after irradiation at low temperature (-25 ± 5°C) to keep the leakage current low. All the irradiated sensors were annealed for 80 minutes at 60°C before the measurements, except for the sensors irradiated to 1×10^{14} and 1×10^{15} n_{eq}/cm^2 that were measured before the annealing. Figure 6 shows the IV curves obtained for the miniature sensors before and after proton irradiations.

Before irradiation, the miniature sensor shows a clear degradation of the breakdown voltage, from > 700 V to 300–400 V, when biased in presence of humidity higher than 41% (figure 6(a)). Similarly, the sensor that received a proton fluence of 1×10^{14} n_{eq}/cm^2 shows a similar degradation of the breakdown voltage, but in this case only when humidity is higher than 51% (figure 6(b)), showing some improvement respect the non-irradiated sensor. The sensor irradiated to 5×10^{14} n_{eq}/cm^2 shows no breakdown below 61%, but a reduction of the breakdown voltage to 350 V is observed for 78% (figure 6(c)). Finally, the sensors irradiated to 1×10^{15} and 2×10^{15} n_{eq}/cm^2 shows no breakdown deterioration even when biased at 69% humidity (figure 6(d) and (e)).

Similarly to the results obtained with full-size sensors, miniature sensors show a degradation of the breakdown voltage when biased at high humidity, but the sensitivity gradually improves when the device accumulates fluence, showing a complete mitigation for fluences above $0.5–1 \times 10^{15}$ n_{eq}/cm^2. However, the humidity needed to deteriorate the breakdown voltage seems to be higher for miniature sensors, confirming less frequent incidence of humidity sensitivity on smaller devices, as suggested in [4].

2023 JINST 18 P02012

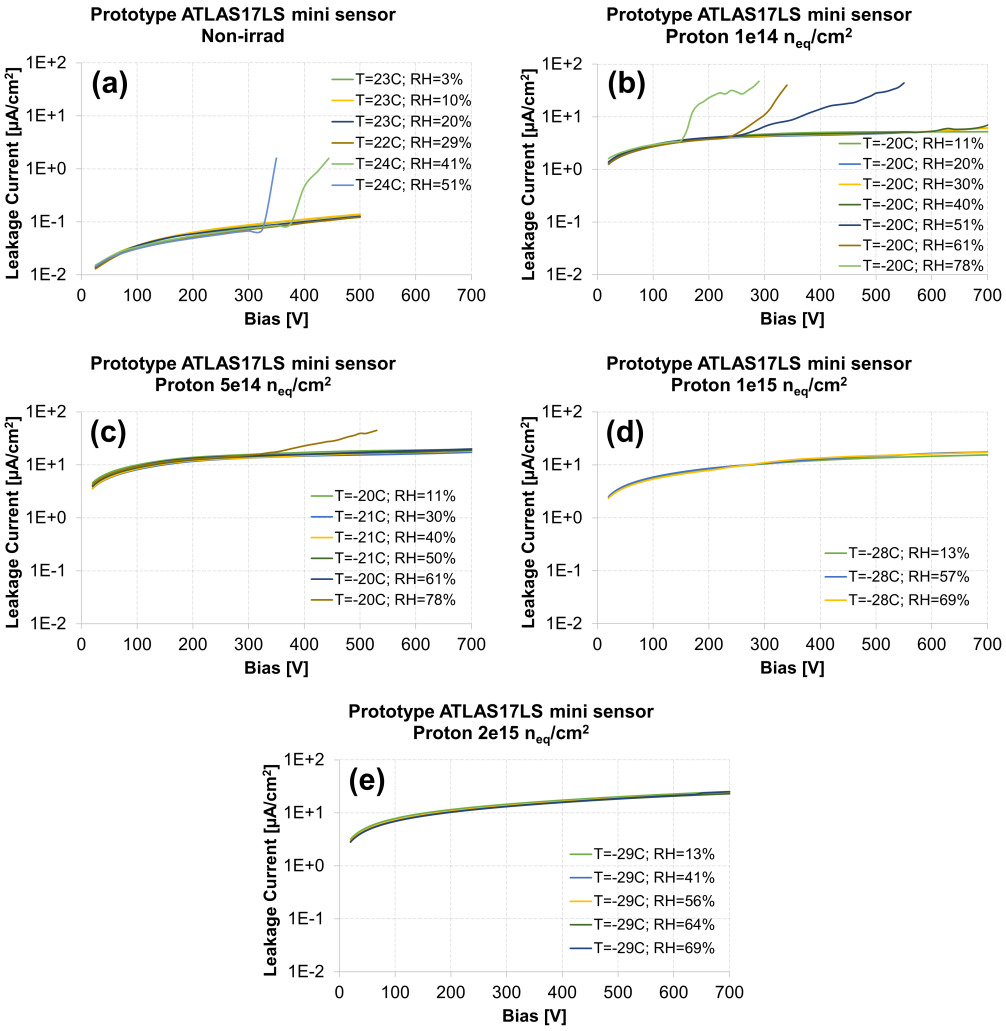

Figure 6. IV curves at different RH for prototype miniature sensors before and after proton irradiations: (a) Non-irradiated, (b) 1×10^{14} n_{eq}/cm^2, (c) 5×10^{14} n_{eq}/cm^2, (d) 1×10^{15} n_{eq}/cm^2 and (e) 2×10^{15} n_{eq}/cm^2.

5 Conclusions

ATLAS ITk full-size strip sensors with different surface properties have been tested at different humidity conditions, showing different levels of breakdown voltage deterioration. Although none of them mitigated completely the humidity sensitivity, thicker passivation layers and p-spray treatments helped to improve considerably the performance of the sensor, showing higher breakdown voltages at high humidity. These results seem to confirm the hypothesis made in previous studies, suggesting that thicker passivation layers can reduce the influence of the positive charges, accumulated on the surface in presence of humidity, in the creation of conducting electron/hole inversion/accumulation layers in the silicon-oxide interface between the guard ring and the edge, that can reduce the breakdown voltage of the device. Similarly, the presence of p-spray can reduce the accumulation of positive charges on the surface, also helping to avoid the appearance of conducting channels. Simulation studies using realistic TCAD model should help to confirm these hypothesis.

2023 JINST 18 P02012

A subset of these sensors were irradiated with protons and neutrons+gammas, showing less sensitivity to humidity variations for higher fluences. These results confirm that in working conditions the humidity sensitivity will be reduced by the radiation effects, and mitigated eventually for fluences above 1×10^{15} n_{eq}/cm^2. Irradiated sensors with different surface properties showed very similar leakage current values, confirming that thicker passivation layers or p-spray addition do not have an impact on the device leakage current.

Additionally, miniature sensors fabricated during the prototyping phase were also studied before and after proton irradiation. The results confirm the progressive reduction of the humidity sensitivity when the sensors accumulate fluence, and the eventual mitigation above $0.5–1 \times 10^{15}$ n_{eq}/cm^2. However, the humidity needed to deteriorate the breakdown is higher than for full-size sensors, confirming less sensitivity on smaller devices, and suggesting that the magnitude of the effect could be proportional to the surface exposed to ambient humidity conditions.

Finally, all the full-size sensors (pre- and post-irradiation) were exposed unbiased to high humidity several days, showing a fast and complete recovery of the breakdown voltage when measured again in dry conditions. These results confirm that there is little risk of permanent deterioration when unbiased sensors are exposed to ambient humidity, as expected during module/petal assembly and detector integration for the HL-LHC upgrade.

Acknowledgments

We gratefully acknowledge Y. Abo, S. Kamada, K. Yamamura, and the team of engineers of HPK for their highly productive work on the designs, layouts, close communication and collaboration. The work at Carleton University, Simon Fraser University (SFU), TRIUMF, and University of Toronto was supported by the Canada Foundation for Innovation and the Natural Science and Engineering Research Council of Canada. The work at Centro Nacional de Microelectrónica (IMB-CNM, CSIC) is part of the Spanish R&D grant PID2019-110189RB-C22, funded by MCIN/AEI/10.13039/501100011033. The work at Santa Cruz Institute for Particle Physics (SCIPP) was supported by the US Department of Energy, grant DE-SC0010107. The work in Prague was supported by the Ministry of Education, Youth and Sports of the Czech Republic coming from the projects LTT17018 Inter-Excellence and LM2018104 CERN-CZ and by Charles University grant GAUK 942119. We acknowledge the support provided by the gamma irradiation facility UJP, Praha, a. s. (Czech Republic). The authors would also like to thank the crew at the TRIGA reactor in Ljubljana for help with the irradiation of the detectors. The Authors acknowledge the financial support from the Slovenian Research Agency (research core funding No. P1_0135).

References

[1] ATLAS collaboration, *The ATLAS Experiment at the CERN Large Hadron Collider*, 2008 *JINST* **3** S08003.

[2] ATLAS collaboration, *Technical Design Report for the ATLAS Inner Tracker Strip Detector*, Tech. Rep., CERN-LHCC-2017-005, CERN, Geneva (2017).

[3] L. Rossi and O. Brüning, *High Luminosity Large Hadron Collider: A description for the European Strategy Preparatory Group*, Tech. Rep., CERN-ATS-2012-236, CERN, Geneva (2012).

2023 JINST 18 P02012

[4] J. Fernández-Tejero et al., *Humidity sensitivity of large area silicon sensors: Study and implications*, *Nucl. Instrum. Meth. A* **978** (2020) 164406.

[5] ATLAS collaboration, *Strip sensor performance in prototype modules built for ATLAS ITk*, *Nucl. Instrum. Meth. A* **978** (2020) 164402.

[6] Y. Unno, H. Abidi, A. Affolder et al., *Specifications and Pre-production of n^+-in-p Large-format Strip Sensors fabricated in 6-inch Silicon Wafers, ATLAS18, for Inner Tracker of ATLAS Detector for High-Luminosity Large Hadron Collider*, *Presented at 23rd International Workshop for Radiation Imaging Detectors*, Riva del Garda, Italy, 26–30 June 2020 [https://indico.cern.ch/event/1120714/contributions/4867100/] [submitted for publication in JINST].

[7] ATLAS collaboration, *Technical Specification for the Supply of Silicon Sensors for the ATLAS Inner Tracker upgrade project*, Tech. Rep., AT2-IS-ED-0014, CERN, Geneva (2019).

[8] Y. Unno et al., *ATLAS17LS – A large-format prototype silicon strip sensor for long-strip barrel section of ATLAS ITk strip detector*, *Nucl. Instrum. Meth. A* **989** (2021) 164928.

2023 JINST 18 P02012